

Diffusion–Thermo and Radiation Absorption on MHD Free Convection Flow of Casson Fluid Past a Vertical Surface With Convective Boundary Condition

G.Vinod Kumar, R.V. M. S. S. Kiran Kumar, P.Durga Prasad

and

S.V. K. Varma

Department of Mathematics

S.V. University, Tirupati-517502, A.P, India

Email: gvkphd@gmail.com, kksaisiva@gmail.com,

durga.prsd@gmail.com,svijayakumarvarma@yahoo.co.in

(Received August 27, 2017)

Abstract: The effects of Diffusion – thermo on MHD free convection flow of a Casson fluid over a vertical preamble surface with the heat source is investigated by introducing convective boundary condition at the surface where the thermal conductivity of the fluid varies linearly with respect to the temperature. Casson fluid model is used to characterize the non-Newtonian fluid behaviour. The governing partial differential equations are converted into non-linear ordinary differential equations by using similarity transformation and the expressions for the velocity, temperature and concentration distributions are obtained using perturbation technique. The behaviour of flow quantities within the boundary layer has been discussed and analyzed for various flow parameters through graphs. The influence of the Skin-friction, the local Nusselt number and the local Sherwood number is discussed and presented in tabular form.

Keywords: Casson fluid, convective boundary condition, porous medium, radiation absorption, chemical reaction.

1. Introduction

The flow of non-Newtonian fluids is applied in many situations in industry such as processing of materials and chemical engineering. These fluids show different characteristics from the Newtonian fluids which cannot be fully represented by the Navier-Stokes equations. To represent

these non-Newtonian fluids some modifications to the Navier-Stokes equations are used and these are seen in many research works which studied viscoelastic and micropolar fluids¹⁻². These fluids are categorized as viscoelastic, thixotropic, and power-law fluids. The constitutive equations of such fluids cannot fully represent the actual behaviour of these fluids. These fluids include contaminated lubricants, molten metal, synovial fluids, etc. Many fluids used in industries show non-Newtonian behaviour, so the modern day researchers are more interested in those industrial non-Newtonian fluids and their dynamics. A single constitutive equation is not enough to cover all properties of such non-Newtonian fluids and hence many non-Newtonian fluid models³⁻⁶ have been proposed to clarify all physical behaviours. Casson fluid is one of the types of such non-Newtonian fluids, which behaves like an elastic solid, and for this fluid, a yield shear stress exists in the constitutive equation. Casson fluid can be defined as a shear thinning liquid which is presumed to have an infinite viscosity at zero rate of shear and a yield stress under which no flow occurs and zero viscosity at an infinite rate of shear. Casson fluid model is used in many foodstuffs and biological materials, especially blood. It describes the steady shear stress, shear rate behaviour of blood. Merrill et al.⁷ and Mac Donald⁸ investigate the behaviour of blood.

The study of magnetohydrodynamic (MHD) flow of non-Newtonian fluid in a porous medium has attracted the attentions of many researchers. Of course, it is due to the fact that such phenomena are mostly found in the optimization of solidification processes of metals and metal alloys, the geothermal sources investigation and nuclear fuel debris treatment. However, non-Newtonian fluids are subtle compare to Newtonian fluids. Indeed, the resulting equations of non-Newtonian fluids give highly nonlinear differential equations which are usually difficult to solve. These equations add further complexities when MHD flows in a porous space have been taken into account. Simple applications for the MHD flows of non-Newtonian fluids in a porous medium are encountered in irrigation problems, heat-storage beds, and biological systems, process of petroleum, textile, paper and polymer composite industries. Numerous studies have been presented on various aspects of MHD flows of non-Newtonian fluid flows passing through a porous medium. One may refer to some recent investigations⁹⁻¹³. The heat transfer aspects of the Casson fluid flow is an important research area due to its relevance to the optimized processing of chocolate, toffee and other foodstuffs¹⁴. Recently, Akbar and Khan¹⁵ studied the metachronal beating of cilia under the influence of Casson fluid and magnetic field. The unsteady MHD free flow of a Casson fluid past an

oscillating vertical plate with constant wall temperature. The fluid is electrically conducting and passing through a porous medium analyzed by Asma Khalid¹⁶⁻¹⁷. Mustafa et al.¹⁸ studied the unsteady boundary layer flow and heat transfer of a Casson fluid over a moving flat plate with a parallel free stream using the Homotopy Analysis Method. Casson fluid flow over a vertical porous surface with chemical reaction in the presence of magnetic field has been studied by Arthur¹⁹.

The energy flux caused by a composition gradient is called Dufour or diffusion-thermal effect. Generally, the thermal-diffusion and the diffusion thermo effects are of smaller order of magnitude than the effects prescribed by Fick's laws and are often neglected in heat and mass transfer processes by many researchers. Mukhopadhyay²⁰. Hayat et al.²¹ investigated Soret and Dufour effects on magnetohydrodynamic (MHD) flow of Casson fluid. In all of the above mentioned studies, fluid viscosity and fluid thermal conductivity was assumed to be constant within the boundary layer. Sharada²² analyzed the mixed convection flow of a Casson fluid over an exponentially stretching sheet with the effects of Soret and Dufour, thermal radiation, chemical reaction effects.

Motivated by the previously mentioned investigations on flow of non-Newtonian fluids over a vertical plate and its vast applications in many industries, in the present paper, the unsteady two-dimensional MHD flow of electrically conducting non-Newtonian Casson fluid, heat and mass transfer in presence of diffusion thermo and radiation absorption effects with convective boundary condition is investigated.

2. Mathematical Formulation

Consider the unsteady free convective heat and mass transfer flow of a laminar, viscous, electrically conducting, heat absorbing and chemically reactive Casson fluid past a semi infinite vertical permeable moving plate embedded in a uniform porous medium in the presence of thermal and concentration buoyancy effects. A Uniform magnetic field of strength B_0 is applied in the perpendicular direction towards the flow also the induced magnetic Reynolds number which is taken to be very small. The first order chemical reactions are taking place in the flow. The unsteady fluid and heat flows start at $t = 0$.

The rheological equation an incompressible and isotropic Casson fluid, reported by Casson is

$$\tau = \tau_0 + \mu\alpha$$

$$\tau_{ij} = \begin{cases} 2 \left(\mu_{\beta} + \frac{P_y}{\sqrt{2\pi}} \right) e_{ij}, & \pi > \pi_c \\ 2 \left(\mu_{\beta} + \frac{P_y}{\sqrt{2\pi_c}} \right) e_{ij}, & \pi < \pi_c \end{cases}$$

Where τ, τ_0, μ and α are, respectively shear stress, Casson yield stress, dynamic viscosity shear rate and $\pi = e_{ij}e_{ij}$ and e_{ij} is the $(i, j)^{th}$ component of deformation on rate, π_c is the critical value of this product, μ_{β} is plastic dynamic viscosity of the non-Newtonian fluid, and P_y denote the yield stress of the fluid. Under above assumptions mode, the governing equations of such type of flow are given by

$$(2.1) \quad \frac{\partial v}{\partial y} = 0,$$

$$(2.2) \quad \frac{\partial u^*}{\partial t^*} + \mathcal{G}^* \frac{\partial u^*}{\partial y^*} = \nu \left(1 + \frac{1}{\beta} \right) \frac{\partial^2 u^*}{\partial y^{*2}} - \left(\frac{\sigma B_0^2}{\rho} + \frac{\nu}{K^*} \right) u^* + g\beta_T (T^* - T_{\infty}) u^* + g\beta_c (C^* - C_{\infty}),$$

$$(2.3) \quad \frac{\partial T^*}{\partial t^*} + \mathcal{G}^* \frac{\partial T^*}{\partial y^*} = \frac{\kappa}{\rho c_p} \frac{\partial^2 T^*}{\partial y^{*2}} - \frac{Q_0}{\rho c_p} (T^* - T_{\infty}) + \frac{Q_l^*}{\rho c_p} (C^* - C_{\infty}) + \frac{D_m \kappa_T}{C_s C_p} \frac{\partial^2 c^*}{\partial y^{*2}},$$

$$(2.4) \quad \frac{\partial C^*}{\partial t^*} + \mathcal{G}^* \frac{\partial C^*}{\partial y^*} = D \frac{\partial^2 C^*}{\partial y^{*2}} - K_l (C^* - C_{\infty}),$$

Where u^*, v^* are the components of dimensional velocities along x^* and y^* directions, respectively, t^* is the dimensional time, β is the Casson fluid

parameter, C^* is the dimensional concentration, C_w and T_w are the wall concentration and wall temperature. C_∞ and T_∞ are the ambient concentration and temperature of the fluid. ρ is the fluid density, ν is the kinetic viscosity, c_p is the specific heat at the constant pressure, σ is the electrical conductivity of the fluid, B_0 is the magnetic induction, K^* is the permeability of the porous medium, Q_0 is the dimensional heat absorption coefficient, Q_1^* is the coefficient of proportionality for the absorption of the radiation, D is the mass diffusivity, g is the gravitational acceleration, β_T and β_c are the thermal and concentration expansion coefficients, respectively and K_1 is the first order chemical reaction coefficient. The approximate boundary conditions for the velocity, temperature and concentration fields are

$$(2.5) \quad \begin{aligned} u^* &= u_p^*, \quad -k \frac{\partial T}{\partial y} = h(T_w - T_\infty), \quad \text{at } y = 0, \\ C^* &= C_w + \varepsilon (C_w - C_\infty) e^{n^* t^*} \quad \text{at } y^* = 0, \quad , \quad \text{at } y^* = 0 \\ u^* &= 0, \quad T^* \rightarrow T_\infty, \quad C^* \rightarrow C_\infty, \quad \text{as } y^* \rightarrow \infty \end{aligned}$$

Where u_p^* is the wall dimensional velocity, n^* is constant. It is clear from Eq.(2.1) that the suction velocity at the plate surface is a function of the time only. Assuming that it takes the following exponential form:

$$(2.6) \quad \mathcal{G}^* = -V_0 \left(1 + \varepsilon A e^{n^* t^*} \right),$$

Where A is small real positive real constant, ε and εA are small and less than unity, V_0 is scale of the suction velocity which has non-zero positive constant. On introducing the dimensionless quantities.

$$(2.7) \quad \begin{aligned} u &= \frac{u^*}{V_0}, \quad \mathcal{G} = \frac{\mathcal{G}^*}{V_0}, \quad y = \frac{V_0 y^*}{\nu}, \quad t = \frac{V_0 t^*}{\nu}, \quad n = \frac{n^* \nu}{V_0^2}, \\ \theta &= \frac{T^* - T_\infty}{T_w - T_\infty}, \quad C = \frac{C^* - C_\infty}{C_w - C_\infty}, \end{aligned}$$

In the view of the above non-dimensional variables, the basic fields Eqs.(2.2)-(2.4) can be expressed in non-dimensional form as

$$(2.8) \quad \frac{\partial u}{\partial t} - (1 + \varepsilon A e^{nt}) \frac{\partial u}{\partial y} = \left(1 + \frac{1}{\beta}\right) \frac{\partial^2 u}{\partial y^2} - \left(M + \frac{1}{K}\right) u + Gr\theta + GrC$$

$$(2.9) \quad \frac{\partial \theta}{\partial t} - (1 + \varepsilon A e^{nt}) \frac{\partial \theta}{\partial y} = \frac{1}{Pr} \frac{\partial^2 \theta}{\partial y^2} = \phi\theta + Q_l C + Du \frac{\partial^2 C}{\partial y^2}$$

$$(2.10) \quad \frac{\partial C}{\partial t} - (1 + \varepsilon A e^{nt}) \frac{\partial C}{\partial y} = \frac{1}{Sc} \frac{\partial^2 C}{\partial y^2} - KrC$$

The boundary conditions are

$$(2.11) \quad \begin{aligned} u &= u_p, \theta' = -\gamma_1(1 - \theta(0)), C = 1 + \varepsilon e^{nt}, \text{ on } y = 0 \\ u &\rightarrow 0, \theta \rightarrow 0, C \rightarrow 0 \text{ as } y \rightarrow \infty \end{aligned}$$

Where Gr is the Grashof number, Gm is the solutal Grashof number, Pr is the Prandtl number, M is the magnetic field parameter, K is the permeability parameter, Kr is the chemical reaction parameter, Sc is the Schmidt number, ϕ is the heat source parameter and Q_l is the absorption of radiation parameter, γ_1 is the convective parameter.

$$\begin{aligned} Gr &= \frac{\nu g \beta (T_w - T_\infty)}{V_0^3}, \quad Gm = \frac{\nu g \beta_c (C_w - C_\infty)}{V_0^3}, \quad Pr = \frac{\mu c_p}{\kappa}, \quad M = \frac{\sigma B_0^2 \nu}{\rho V_0^2}, \\ K &= \frac{K^* V_0^2}{\nu^2}, \quad Kr = \frac{K_l \nu}{V_0^2}, \quad Sc = \frac{\nu}{D}, \quad \phi = \frac{Q_0 \nu}{\rho c_p V_0^2}, \quad Q_l = \frac{\nu^2 Q_l^* (C_w - C_\infty)}{(T_w - T_\infty) V_0^2 k}, \\ Du &= \frac{D_m k_T (C_w - C_\infty)}{C_s C_\nu \nu (T_w - T_\infty)}, \end{aligned}$$

The mathematical statement of above problem is completed and embodies the solution of Eqs.(2.8)-(2.10) subject to boundary condition (2.11)

3. Method of Solution

Eqs. (2.8) - (2.10) represents a set of partial differential equations that cannot be solved in enclosed form. However, it can be reduced to a set of ordinary differential equations in dimensionless form that can be solved analytically this can be done by representing the velocity, temperature and the concentration as

$$(3.1) \quad \begin{aligned} u(y,t) &= u_0 + \varepsilon e^{nt} u_1(y) + O(\varepsilon^2), \\ \theta(y,t) &= \theta_0 + \varepsilon e^{nt} \theta_1(y) + O(\varepsilon^2), \\ C(y,t) &= C_0 + \varepsilon e^{nt} C_1(y) + O(\varepsilon^2), \end{aligned}$$

Substituting Eqs. (3.1). Into (2.8)–(2.10) equating the harmonic and non-harmonic terms, and neglecting the higher order of $O(\varepsilon^2)$, and simplifying we obtain the following pairs of equation u_0, θ_0, C_0 and u_1, θ_1, C_1

$$(3.2) \quad \left(1 + \frac{1}{\beta}\right) u_0'' + u_0' + \left(M + \frac{1}{K}\right) u_0 = -Gr\theta_0 - GmC_0$$

$$(3.3) \quad \theta_0'' + Pr\theta_0' - Pr\phi\theta_0 = -Q_l Pr C_0 - Pr DuC_0''$$

$$(3.4) \quad C_0'' + ScC_0' - Sc\gamma C_0 = 0$$

Subject to boundary condition

$$(3.5) \quad \begin{aligned} u_0 &= u_p, \theta_0 = 1, C_0 = 1, \text{ on } y=0 \\ u_0 &\rightarrow 0, \theta_0 \rightarrow 0, C_0 \rightarrow 0, \text{ as } y \rightarrow \infty \end{aligned}$$

For first order equations, and

$$(3.6) \quad \left(1 + \frac{1}{\beta}\right) u_1'' + u_1' - \left(M + \frac{1}{K} + n\right) u_1 = -Au_0' - Gr\theta_1 - GmC_1$$

$$(3.7) \quad \theta_1'' + Pr\theta_1' - Pr(\phi + n)\theta_1 = -Pr A\theta_0' - Pr Q_l - Pr DuC_1''$$

$$(3.8) \quad C_1'' + ScC_1'' - Sc(Kr + n)C_1 = -AScC_0'$$

With the boundary conditions

$$(3.9) \quad \begin{aligned} u_1 = 0, \theta_1 = 0, C_1 = 0 \text{ on } y = 0 \\ \theta_1 = 0, C_1 = 0, \text{ as } y \rightarrow \infty \end{aligned}$$

Without going into detail, the solution of Eqns and can be shown

$$(3.10) \quad \begin{aligned} u(y, t) = Le^{-m_3y} - B_2e^{-m_2y} + B_3e^{-m_1y} \\ + \varepsilon e^{nt} (A_6e^{-m_6y} + R_1e^{-m_1y} + A_6e^{-m_6y} - R_2e^{-m_2y} + R_4e^{-m_4y} - R_5e^{-m_5y}) \end{aligned}$$

$$(3.11) \quad \begin{aligned} \theta(y, t) = A_2e^{-m_2y} - B_1e^{-m_1y} \\ + \varepsilon e^{nt} (A_5e^{-m_5y} + B_5e^{-m_5y} + B_6e^{-m_2y} - B_7e^{-m_4y}) \end{aligned}$$

$$(3.12) \quad C(y, t) = e^{-m_1y} + \varepsilon e^{nt} ((1 - B_4)e^{-m_4y} + B_4e^{-m_1y})$$

The physical quantities of interest are the wall shear stress τ_w and the local surface heat transfer rate

$$(3.13) \quad \tau_w = \mu \left(1 + \frac{1}{\beta} \right) \frac{\partial u^*}{\partial y^*} \Big|_{y^* = 0} = \rho V_0^2 u'(0)$$

Therefore the local factor C_f is given by

$$(3.14) \quad \begin{aligned} C_f = \frac{\tau_w}{\rho V_0^2} = \left(1 + \frac{1}{\beta} \right) u'(0) \\ = \left(1 + \frac{1}{\beta} \right) \left(\begin{aligned} & -m_3L + m_2B_2 - m_1B_3 + \varepsilon e^{nt} \\ & (-m_6A_6 - m_1R_1 + m_2R_2 - m_3R_3 - m_4R_4 + m_5R_5) \end{aligned} \right) \end{aligned}$$

The local surface heat flux is given by

$$(3.15) \quad q_w = -\kappa \left. \frac{\partial T^*}{\partial y^*} \right|_{y^*=0}$$

Where κ is the effective thermal conductivity, together with the definition of Nusselt number

$$(3.16) \quad Nu_x = \frac{q_w}{T_w - T_\infty} \frac{x}{\kappa}$$

The local Nusselt number is given by

$$(3.17) \quad \frac{Nu}{Re_x} = -\theta'(0) = -m_2 A_2 + m_1 B_1 + \varepsilon e^m (-m_5 A_5 - m_5 B_5 - m_2 B_6 - m_4 B_7)$$

Where $Re_x = \frac{V_0 x}{\nu}$ is the local Reynolds number.

The local Sherwood number is given by

$$(3.18) \quad Sh = -C'(0) = m_1 + \varepsilon e^m [m_4(1 - B_4) + m_1 B_4]$$

4. Results and Discussion

In order to get a physical insight of the problem, the numerical calculations are carried out to illustrate the influence of various physical parameters on the velocity, temperature and concentration are presented graphically in Figures (2.1)-(3.1). Also, the wall Skin-friction coefficient, the rate of heat and mass transfer coefficients are derived and discussed through tables. Throughout the calculations, the parametric values are chosen as: $\varepsilon = 0.02$, $A = 0.5$, $Pr = 0.71$, $t = 1$, $u_p = 0.5$, $n = 0.5$. All the graphs therefore correspond to these values unless specifically indicated on the appropriate graph.

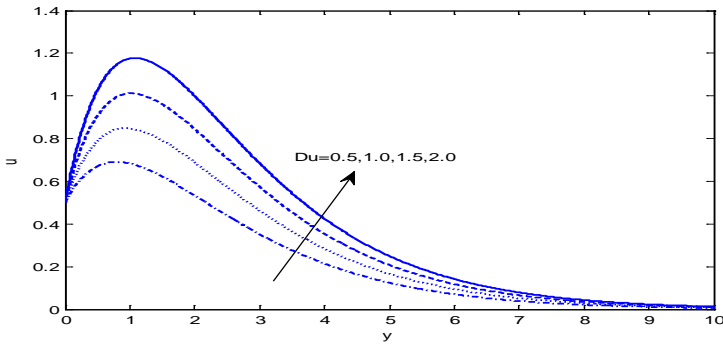


Figure 1: Velocity profiles for Dufour number Du with $Sc = 0.60, Kr = 0.5, \phi = 0.3, \beta = 0.1, Q_l = 0.5, \gamma_1 = 0.2, u_p = 0.5, Gr = 2, Gm = 2, M = 2, K = 0.5$

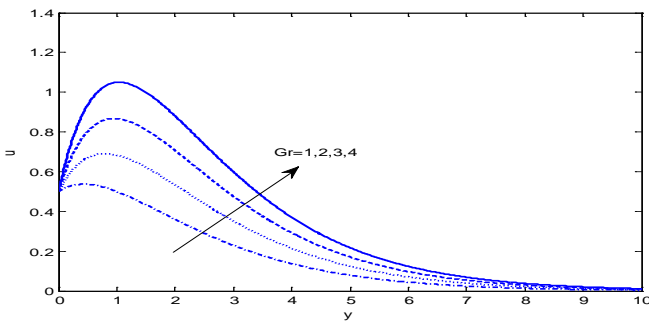


Figure 2: Velocity profiles for Grashof number Gr with $Sc = 0.60, Kr = 0.5, \phi = 0.3, \beta = 0.1, Q_l = 0.5, Du = 0.5, \gamma_1 = 0.2, u_p = 0.5, Gm = 2, M = 2, K = 0.5$

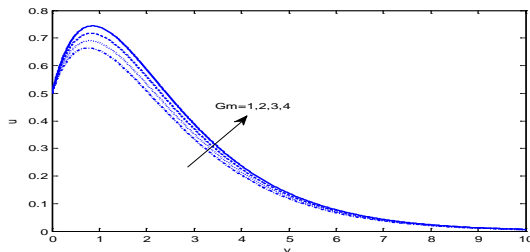


Figure 3: Velocity profiles for Solutal Grashof number Gm with $Sc = 0.60, Kr = 0.5, \phi = 0.3, \beta = 0.1, Q_l = 0.5, Du = 0.5, \gamma_1 = 0.2, Gr = 2, M = 2, K = 0.5$

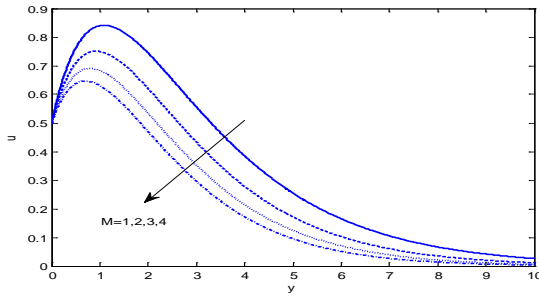


Figure 4: Velocity profiles for magnetic field parameter M with $Sc = 0.60, Kr = 0.5, \phi = 0.3, \beta = 0.1, Q_l = 0.5, Du = 0.5, \gamma_1 = 0.2, Gr = 2, Gm = 2, K = 1$

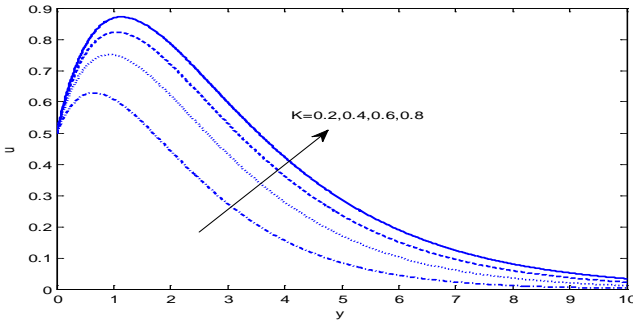


Figure 5: Velocity profiles for permeability parameter K with $Sc = 0.60, Kr = 0.5, \phi = 0.3, \beta = 0.1, Q_l = 0.5, Du = 0.5, \gamma_1 = 0.2, Gr = 2, Gm = 2, M = 0.5$

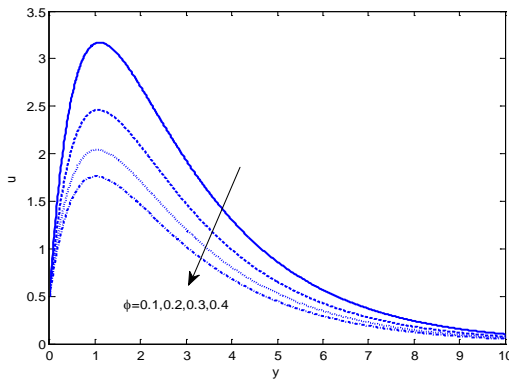


Figure 6: Velocity profiles for heat source parameter ϕ with $Sc = 0.3, Kr = 0.2, \beta = 0.9, Q_l = 2, Du = 0.5, \gamma_1 = 0.2, Gr = 4, Gm = 2, M = 2, K = 0.5$

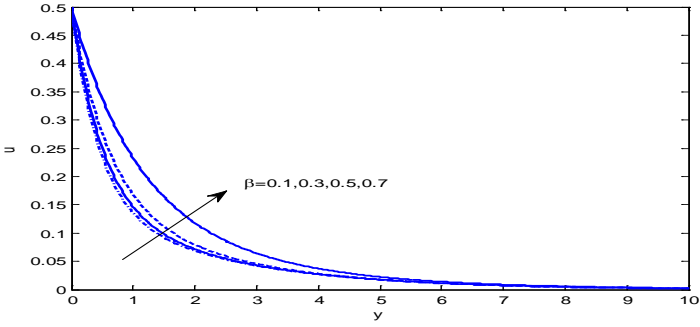


Figure 7: Velocity profiles for Casson fluid parameter β with $Sc = 0.30, Kr = 0.2, \phi = 0.3, Q_l = 0.2, Du = 0.5, \gamma_1 = 0.2, Gr = 1, Gm = 1, M = 0.5, K = 0.1$

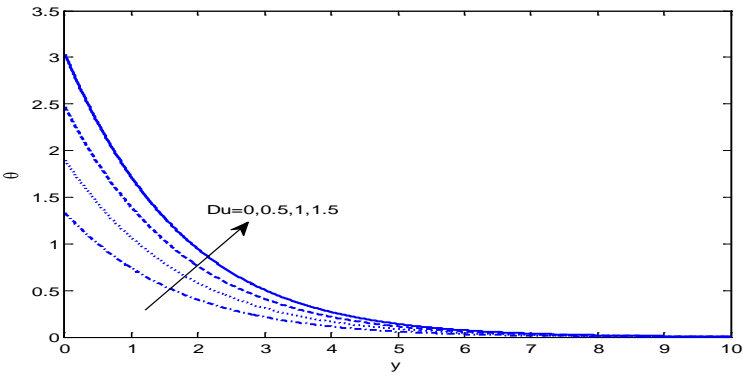


Figure 8: Temperature profiles for different values of Dufour number Du with $Sc = 0.60, Kr = 0.1, \phi = 0.2, Q_l = 0.5, \gamma_1 = 0.2$

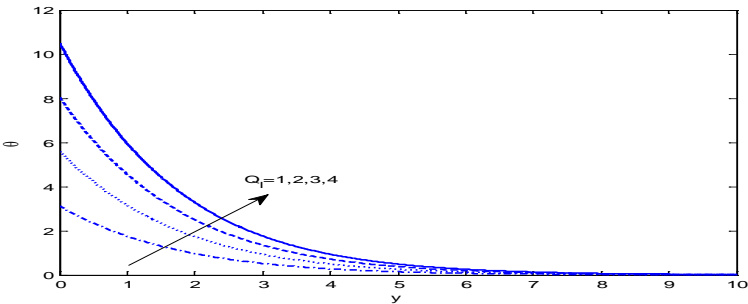


Figure 9: Temperature profiles for different values of radiation absorption parameter Q_l with

$$Sc = 0.60, Kr = 0.1, \phi = 0.2, Du = 0.5, \gamma_1 = 0.2$$

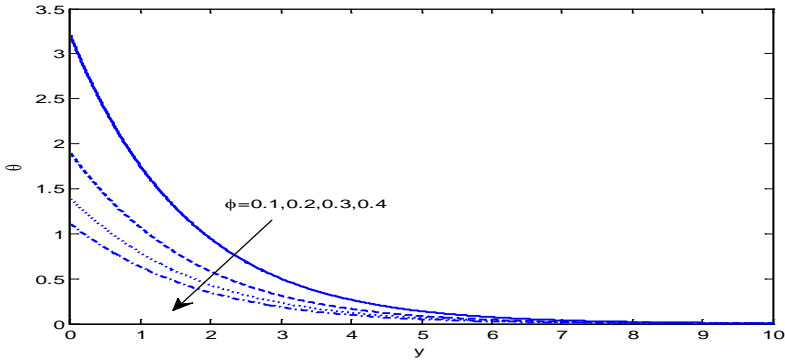


Figure 10: Temperature profiles for different values of heat source parameter ϕ with $Sc = 0.60, Kr = 0.1, Q_1 = 0.5, Du = 0.5, \gamma_1 = 0.2$

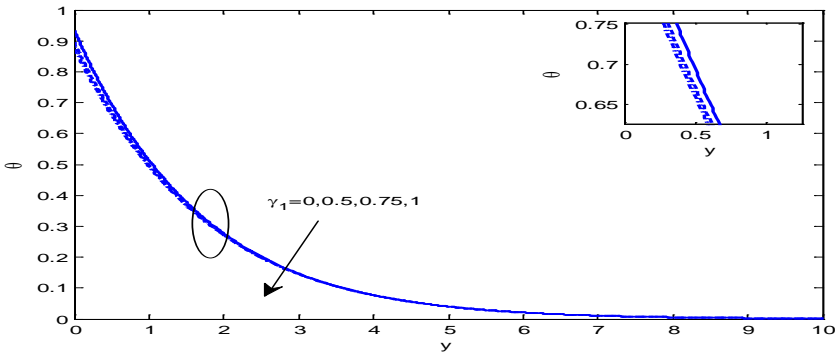


Figure 11: Temperature profiles for different values of convective parameter γ_1 with $Sc = 0.60, Kr = 0.1, \phi = 0.2, Du = 0.5, Q_1 = 0.1$

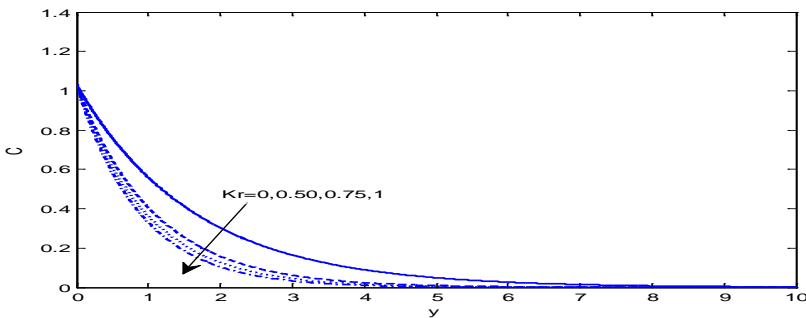


Figure 12: Concentration profiles for different values of chemical reaction parameter Kr with $Sc = 0.60$

Table 1 Numerical values of wall Skin-Friction coefficient for different flow parameters. $Gr = 2, Gm = 2, \gamma_1 = 0.5, t = 1, Sc = 0.30, Pr = 0.71, u_p = 0.5, A = 0.5, n = 0.5, \varepsilon = 0.02$

Kr	γ_1	ϕ	β	Q_l	Du	M	K	Cf
0	0.3	0.2	0.4	0.3	0.3	0.5	0.1	-0.3708
0.2	0.3	0.2	0.4	0.3	0.3	0.5	0.1	-0.4005
0.3	0.3	0.2	0.4	0.3	0.3	0.5	0.1	-0.4047
0.1	0.2	0.2	0.4	0.3	0.3	0.5	0.1	-0.3933
0.1	0.4	0.2	0.4	0.3	0.3	0.5	0.1	-0.3897
0.1	0.6	0.2	0.4	0.3	0.3	0.5	0.1	-0.3871
0.1	0.3	0.3	0.4	0.3	0.3	0.5	0.1	-0.4333
0.1	0.3	0.4	0.4	0.3	0.3	0.5	0.1	-0.4619
0.1	0.3	0.5	0.4	0.3	0.3	0.5	0.1	-0.4828
0.1	0.3	0.2	0.1	0.3	0.3	0.5	0.1	-0.2488
0.1	0.3	0.2	0.2	0.3	0.3	0.5	0.1	-0.3144
0.1	0.3	0.2	0.3	0.3	0.3	0.5	0.1	-0.3583
0.1	0.3	0.2	0.4	0.5	0.3	0.5	0.1	-0.2777
0.1	0.3	0.2	0.4	0.6	0.3	0.5	0.1	-0.2208
0.1	0.3	0.2	0.4	0.7	0.3	0.5	0.1	-0.2208
0.1	0.3	0.2	0.4	0.3	0.5	0.5	0.1	-0.3754
0.1	0.3	0.2	0.4	0.3	1.0	0.5	0.1	-0.3357
0.1	0.3	0.2	0.4	0.3	1.5	0.5	0.1	-0.2960
0.1	0.3	0.2	0.4	0.3	0.3	1.0	0.1	-0.4227
0.1	0.3	0.2	0.4	0.3	0.3	2.0	0.1	-0.4823
0.1	0.3	0.2	0.4	0.3	0.3	3.0	0.1	-0.5380
0.1	0.3	0.2	0.4	0.3	0.3	0.5	0.2	-0.3587
0.1	0.3	0.2	0.4	0.3	0.3	0.5	0.3	-0.2391
0.1	0.3	0.2	0.4	0.3	0.3	0.5	0.4	-0.1716

Table 2 Numerical values of the rate of heat transfer coefficient for various flow parameters. $Sc = 0.30, Pr = 0.71, n = 0.5, A = 0.5, t = 1, \varepsilon = 0.02$

Kr	γ_1	ϕ	Q_l	Du	Nu
0	0.3	0.2	0.3	0.3	0.2587
0.2	0.3	0.2	0.3	0.3	0.3911
0.3	0.3	0.2	0.3	0.3	0.4414
0.1	0.2	0.2	0.3	0.3	0.3324
0.1	0.4	0.2	0.3	0.3	0.3291

0.1	0.6	0.2	0.3	0.3	0.3265
0.1	0.3	0.3	0.3	0.3	0.2817
0.1	0.3	0.4	0.3	0.3	0.2497
0.1	0.3	0.5	0.3	0.3	0.2270
0.1	0.3	0.2	0.5	0.3	0.4700
0.1	0.3	0.2	0.6	0.3	0.5397
0.1	0.3	0.2	0.7	0.3	0.6094
0.1	0.3	0.2	0.3	0.5	0.3527
0.1	0.3	0.2	0.3	1.0	0.4078
0.1	0.3	0.2	0.3	1.5	0.4629

The effect of Dufour number (Du) on tangential velocity distribution is depicted in figure 1. It can be seen that as the Dufour number increase, the tangential velocity increases. Also, it is observed that the thickness of the momentum boundary layer increases with increasing values of Du . The velocity profiles for different values of thermal Grashof number Gr and solutal Grashof number Gm is shown in Figs. 2 and 3. From these figures it is observed that the fluid velocity increases with increasing values of Gr and Gm . The flow is accelerated due to the enhancement in the buoyancy forces. Since the governing equations are coupled together only with the buoyancy parameters, the thermal and solutal Grashof numbers accelerates the fluid so the velocity and the boundary-layer thickness increases with the increase in Gr and Gm . The effect of Magnetic field parameter M is presented in Fig. 4. It is seen that an increasing values of M results into a decrease in the fluid velocity. This is due to the retarding nature of the Lorentz force which slows down the motion of the fluid in the boundary layer. Fig. 5 depict the influence of porous permeability parameter K on velocity profiles. It is observed that the fluid velocity decreases with an increase in the permeability parameter (K). Physically, this refers to the fact that increasing the tightness of the porous medium which is represented by increase in K results in increasing the resistance against the flow. Also, it is seen that velocity reaches the maximum peak value at near the surface. Fig. 6 shows the velocity profiles for different values of dimensionless heat absorption coefficient ϕ , clearly as ϕ increase the peak value of velocity tends to decrease. Physically, the presence of heat absorption coefficient has the tendency to reduce the fluid temperature. This causes the thermal buoyancy effects to decrease resulting in a net reduction in the fluid velocity. Effects of Casson parameter β on velocity is clearly exhibited in Fig. 7. It is noticed that the effect of increasing values of β is to increase the velocity at near the surface, and hence, it reduces far away from the plate. The Dufour effect on the temperature profiles are examined in Fig. 8, it can be seen that the temperature increase with the increase in the Dufour number. Physically, the Dufour term that appears in the temperature equation measures the

contribution of concentration gradient to thermal energy flux in the flow domain. It has a vital role in the ability to increase the thermal energy in the boundary layer. Fig. 9 present the effect of absorption radiation parameter Q_1 on temperature profiles. From this figure it is noticed that the fluid temperature increases with increasing values of Q_1 . This is due to the fact that the large Q_1 values correspond to an increase dominance of conduction over absorption radiation thereby increasing buoyancy force and thickness of the thermal boundary layer. Fig. 10 represents the decrease in fluid velocity when the heat source parameter ϕ is increased it is also observed that the hydromagnetic boundary layer decrease as the heat absorption effect increase. Fig.11 presents typical profiles for temperature distribution for various values of the convective parameter γ_1 . It is seen that the temperature of the fluid field decreases on increasing γ_1 in the boundary layer region and is maximum at the surface of the plate. Thus, by escalating γ_1 , thermal boundary layer thickness enhances. So, we can interpret that the rate of heat transfer decreases with increase in convective parameter γ_1 . Fig.12 depicts the influence of chemical reaction parameter on species concentration. An increase in chemical reaction parameter will suppress the concentration of the fluid. Higher values of Kr amount to a fall in the chemical molecular diffusivity, i.e., less diffusion. Therefore, they are obtained by species transfer. An increase in Kr will suppress species concentration. The concentration distribution decreases at all points of the flow field with the increase in the reaction parameter.

The numerical value skin friction coefficient and the rate of heat transfer coefficient are presented in table 1 and 2. From Table 1 it is seen that skin friction coefficient increases with the increasing values of γ_1, Q_1, Du and K , but the opposite trend is observed with an increase in Kr, ϕ, β and M . Further the rate of heat transfer coefficient increases with the increasing values of Kr, Q_1 and Du , while it decreases with γ_1 and ϕ_1 it is shown in Table 2.

5. Conclusions

The heat and mass transfer with diffusion thermo and radiation absorption effects for an unsteady hydromagnetic boundary layer flow of a non Newtonian Casson fluid past a vertical plate embedded in a porous

medium with convective boundary condition has been studied. In this study, the following remarks can be summarized.

1. The momentum boundary layer thickness increases with Dufour number and Casson parameter.
2. The magnitude of wall skin friction coefficient decreases with Casson parameter.
3. The temperature of the fluid decreases with convective parameter γ_1 . It is also found that the rate of heat transfer decreases with increases γ_1 .
4. Thermal boundary layer thickness with an increase in heat absorption parameter.
5. Rise in distributive chemical reaction parameter ($Kr > 0$) will surprise the concentration of the fluid.

6. Limiting Case

The Casson parameter β is large enough i.e. $\beta \rightarrow \infty$, the non-Newtonian behaviours disappear and the fluid purely behaves like a Newtonian fluid.

Appendix

$$m_1 = \frac{1}{2} \left(Sc + \sqrt{Sc^2 + 4KrSc} \right); m_2 = \frac{1}{2} \left(Pr + \sqrt{Pr^2 + 4Pr\phi} \right);$$

$$m_3 = \frac{1}{2} \left(1 + \frac{\sqrt{1 + 4 \left(1 + \frac{1}{\beta} \right) \left(M + \frac{1}{K} \right)}}{\left(1 + \frac{1}{\beta} \right)} \right); m_4 = \frac{1}{2} \left(Sc - \sqrt{Sc^2 + 4Sc(Kr + n)} \right);$$

$$m_5 = \frac{1}{2} \left(Pr + \sqrt{(Pr)^2 + 4Pr(\phi + n)} \right); m_6 = \frac{1}{2} \left(\frac{1 + \sqrt{1 + 4 \left(1 + \frac{1}{\beta} \right) \left(M + \frac{1}{K} + n \right)}}{\left(1 + \frac{1}{\beta} \right)} \right)$$

$$B_1 = \left(\frac{Q_1 Pr + m_1^2 Pr Du}{m_1^2 - Pr m_1 - Pr \phi} \right); A_2 = \left(\frac{B_1 m_1^3 + \gamma_1 B_1 + \gamma_1}{\gamma_1 m_2} \right)$$

$$B_2 = \left(\frac{GrA_2}{\left(1 + \frac{1}{\beta}\right)m_2^2 - m_2 - \left(M + \frac{1}{K}\right)} \right); B_3 = \left(\frac{GrB_1 - Gm}{\left(1 + \frac{1}{\beta}\right)m_1^2 - m_1 - \left(M + \frac{1}{K}\right)} \right)$$

$$B_4 = \left(\frac{m_1 A Sc}{m_1^2 - Sc m_1 - Sc (Kr + n)} \right); B_5 = \left(\frac{Pr (-Am_1 B_1 - Q_l B_4 - m_1^2 Du)}{m_1^2 - Pr m_1 - Pr (\phi + n)} \right);$$

$$A_4 = (1 - B_4) B_6 = \left(\frac{Pr Am_2 A_2}{m_2^2 - Pr m_2 - Pr (\phi + n)} \right);$$

$$B_7 = \left(\frac{(Q_l Pr + m_4^2 Pr Du)(B_4 - 1)}{m_4^2 - Pr m_4 - Pr (\phi + n)} \right)$$

$$A_5 = \left(\frac{\gamma_1 (B_5 + B_6 - B_7) + B_5 m_1 + B_6 m_2 - B_7 m_4}{m_5 + \gamma_1} \right); L = up + B_2 + B_3$$

References

1. P. V. Ramachandra, R. A. Subba, and B. O. Anwa, Flow and heat transfer of Casson fluid from a horizontal cylinder with partial slip in non-Darcy porous medium, *Appl. Comput. Math.*, **2** (2013), 1-2.
2. K. Vajravelu and S. Mukhopadhyay, Diffusion of chemically reactive species in Casson fluid flow over an unsteady permeable stretching surface, *J. Hydrodyn.*, **25** (2013), 591-598.
3. W. L. Wilkinson, The drainage of a maxwell liquid down a vertical plate, *The Chemical Engineering Journal*, **1**(1970), 255–257.
4. K. R. Rajagopal, Viscometric flows of third grade fluids, *Mechanics Research Communications*, **7** (1980), 21–25.
5. K. R. Rajagopal, T. Y. Na, and A. S. Gupta, Flow of a viscoelastic fluid over a stretching sheet, *Rheologica Acta*, **23** (1984), 213–215.
6. C. Doria and J. Tichy, Behavior of a bingham-like viscous fluid in lubrication flows, *Journal of Non-Newtonian Fluid Mechanics*, **45** (1992), 291–310.
7. F. W. Merrill, Rheology of Human Blood and Some Speculations on Its Role in Vascular Homeostatics Biomechanical Mechanisms in Vascular Homeostatics and

- Intravascular Thrombosis. In: Sawyer On Study Flow through Modelled Vascular Stenoses, *Journal of Biomechanics*, **12** (1979), 13-20.
8. S. Nadeem, RizwanUIHaq, N.S. Akbar and Z. H. Khan, MHD three-dimensional Casson fluid flow past a porous linearly stretching sheet, *Alexandria Eng.*, **52** (2013).
 9. A. Mehmood, A. Ali and T. Mahmood, Unsteady magnetohydrodynamic oscillatory flow and heat transfer analysis of a viscous fluid in a porous channel filled with a saturated porous medium, *J. Porous Media*, **13** (2010).
 10. T. M. Eldabe Nabil, M. Moatimid Galal, and S.M. Hoda Ali, Magnetohydrodynamic flow of non-Newtonian visco-elastic fluid through a porous medium near an accelerated plate, *Can. J. Phys.*, **81** (2003).
 11. T.M. Eldabe Nabil and S. N. Sallam, Non-Darcy couette flow through a porous medium of magnetohydrodynamic visco-elastic fluid with heat and mass transfer, *Can. J. Phys.*, **83** (2005).
 12. M. Hameed and S. Nadeem, Unsteady MHD flow of a non-Newtonian fluid on a porous plate, *J. Math. Anal. Appl.*, **325** (2007).
 13. S. Kim, A study of non-Newtonian viscosity and yield stress of blood in a scanning capillary-tube Rheometer, PhD thesis, Drexel University, 2002.
 14. N.S. Akbar and Z. H. Khan, Metachronal beating of cilia under the influence of Casson fluid and magnetic field, *J. Magnet. Magn.Mater.*, **378** (2015), 320–326.
 15. A. Khalid, I. Khan and S. Shafiel, Exact solutions for unsteady free convection flow of a Casson fluid over an oscillating vertical plate with constant wall temperature, *Abstr. Appl. Anal.*, **15** (2015).
 16. Asma Khalid , Ilyas Khan Arshad Khan and Sharidan Shafie, Unsteady MHD free convection flow of Casson fluid past over an oscillating vertical plate embedded in a porous medium, *Engineering Science and Technology, an International Journal*, **18** (2015), 309-317.
 17. M. Mustafa, T. Hayat, I. Pop and Aziz, A. Unsteady Boundary Layer Flow of a Casson Fluid Due to an Impulsively Started Moving Flat Plate, *Heat Transfer-Asian Research*, **40** (2011), 563-576.
 18. Emmanuel Maurice, Ibrahim Yakubu Seini and Letis Bortey Borttei. Analysis of Casson Fluid Flow over a Vertical Porous Surface with Chemical Reaction in the Presence of Magnetic Field, *Journal of Applied Mathematics and Physics*, **3** (2015), 713-723.
 19. S. Mukhopadhyay, Casson fluid flow and heat transfer over a nonlinearly stretching surface, *Chin Phys B*, **22** (2013).
 20. T. Hayat, S. A. Shehzadi and A. Alsaedi, Soret and Dufour effects on magnetohydrodynamic (MHD) flow of Casson fluid, *Appl Math Mech (English Ed.)*, **33** (2012), 1301–12.
 21. K. Sharada and B. Shankar, MHD Mixed Convection Flow of a Casson Fluid over an Exponentially Stretching Surface with the Effects of Soret, Dufour, Thermal Radiation and Chemical Reaction, *World Journal of Mechanics*, **5** (2015), 165-177.